Coupling between fragment radial motion and the transversal degrees of freedom in cold fission

Ş. Mişicu,[1] A. Săndulescu,[1,2] and W. Greiner[1]
[1]*Institut für Theoretische Physik, Johann Wolfgang von-Goethe Universität, Robert-Mayer-Strasse 8-10, D-60325 Frankfurt am Main, Germany*
[2]*National Institute for Nuclear Physics, P.O. Box MG6, Bucharest, Romania*
(Received 23 April 2001; published 24 September 2001)

The tunneling of a quasibound dinuclear system along the main radial mode is studied for the case of cold fission when the very small excitation energy present in the decaying system is distributed among molecular type transversal collective degrees of freedom. Such a collective mode has typical oscillation periods much smaller than the tunneling time of the main radial mode and, therefore, we discuss various approaches that are suitable in dealing with this problem. The modified penetrabilities are obtained at first by solving the coupled set of Schrödinger equations in the adiabatic and the diabatic approximations. The comparison with the one-dimensional penetrability is done also in the frame of the Feynman path integral formalism for a very large inertial mass and small transversal vibrations frequency. In all cases the coupling of the radial(fission) mode to the transversal degrees of freedom leads to a change in the tunneling probability that is, however, not so strong to determine significant variations in the fission lifetime.

DOI: 10.1103/PhysRevC.64.044610 PACS number(s): 25.85.Ca, 21.60.Gx, 24.75.+i

I. INTRODUCTION

Recent years have testified to an increased interest in the experimental investigation of the cold fission process using large Ge detector arrays, such as Gammasphere and Eurogam. These setups enable the identification of gamma rays from individual fission fragments of rare processes such as cold binary and ternary fragmentations of ^{252}Cf through triple gamma coincidence technique [1]. As a result, the yields for cold binary and ternary fission were extracted from intensities of γ rays emitted during the deexcitation of primary fragments (prior to the emission of neutrons). Based on a cluster model in which the tunneling is treated only along a single coordinate, i.e., the radial one (the effect of fragments deformations is included in the potential), a partially satisfactory agreement with the experimental data for the binary cold fission of ^{252}Cf has been obtained [2].

Data have also been reported on the spin distribution of the fission fragments, the first data on rotational states population in the cold fission of ^{252}Cf being published in Ref. [3]. Moreover, the average angular momentum for the primary fission fragments was extracted for different charge splits [4]. Towards the cold fission limit, i.e., for very small excitation energies, the experimental data for even-even fragments, which are providing very small values of the angular momenta, were compared with the results of a theoretical model, which assumes the formation of the angular momentum at the scission point, before the system enters in the penetration regime [5]. The mechanism responsible for the generation of angular momentum in low-energy fission, according to the above-mentioned reference and older studies [6,7] are the bending vibrations. Unconstrained rotations of the fragments before the tunneling is terminated seem to be unlikely in view of the high barriers in the direction perpendicular to the fission axis. A very recent model of angular momentum generation in which fragments are allowed to evolve as individual rotators before the fragments are running in the reciprocal Coulomb field, overestimates sensitively the experimental values [8]. Due to the low excitation energy present in the system, it appears that during tunneling the main degrees of freedom that are interfering with the radial motion are the bending vibrations.[1] More specifically the fission path, or the most probable escape trajectory that minimizes the action S, is centered around the symmetry axis of both fragments such that the penetration is maximized [10]. Displacements perpendicular to the radial direction are stable.

In this paper we consider the planar motion of a dinuclear system, formed from the clusterization of the mother nucleus ^{252}Cf in two fragments and solve the Schrödinger equation of the radial mode, with account of the transversal vibrations, in the one- and n-coupled-channels case assuming an adiabatic and a diabatic coupling, respectively, between these degrees of freedom. A path-integral approach allows us, under certain approximations, to obtain in closed form the total penetrability without being forced to truncate after a definite number of channels like in the coupled-channel case. We present numerical calculations of the penetrabilities taking as an example the experimentally observed cold splitting of ^{252}Cf in two deformed even-even clusters.

II. FISSION DYNAMICS OF THE DINUCLEAR MOLECULE

Like in previous papers [2,3,5] we adopt a cluster(molecular) model to describe the binary fission. In this model the fragments are preformed in their ground states, or very close to it, and together they are trapped in a quasi-bound state, as a consequence of the interplay of heavy-ion nuclear and Coulomb forces. The breakup of this two-body system is described as the decay of a metastable state from the molecular pocket to the Coulomb continuum.

Similar to Ref. [5] we assume that the motion of the fis-

[1]The β vibrations of the fragments are rather weakly coupled to the relative motion [9] and, therefore, are neglected in our further considerations.

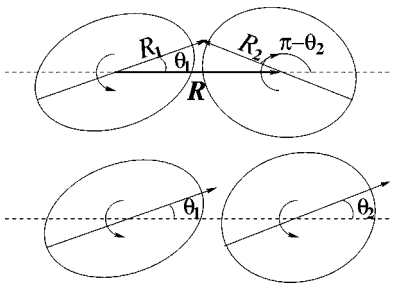

FIG. 1. Dinuclear nonaxial geometry in cold fission: The symmetry axes of the two clusters are making the angles θ_1 and $\pi - \theta_2$, respectively, with the axis joining the centers of the two fragments for *butterfly* configuration (upper part) and the angles θ_1 and θ_2 for the *antibutterfly* configuration (lower part).

sion fragments is confined within the plane. Eliminating the c.m. motion and using the angular momentum conservation, the classical Hamiltonian of the dinuclear molecule reads

$$H=\frac{1}{2}\mu\dot{R}^2+\frac{1}{2}\left(\frac{1}{J_1}+\frac{1}{\mu R^2}\right)L_1^2+\frac{1}{2}\left(\frac{1}{J_2}+\frac{1}{\mu R^2}\right)L_2^2 + \frac{1}{\mu R^2}L_1L_2+V(R,\theta_1,\theta_2), \tag{1}$$

where $L_i=J_i\dot{\theta}_i$ is the ith fragments angular momenta, θ_i is the angle between the fission axis and the symmetry axis of the fragment i, and J_i is its moment of inertia (see Fig. 1). The coordinate describing the fission mode in a molecular model is the interfragment distance R that is analogous to the elongation variable in a hydrodynamical model of spontaneous fission [11].

Upon quantization (see for details, Ref. [12]) we obtain the following expression for the kinetic-energy operator:

$$\hat{T}=-\frac{\hbar^2}{2\mu}\frac{\partial^2}{\partial R^2}-\frac{\hbar^2}{2\mathcal{B}_1(R)}\frac{\partial^2}{\partial\theta_1^2}-\frac{\hbar^2}{2\mathcal{B}_2(R)}\frac{\partial^2}{\partial\theta_2^2} + \frac{\hbar^2}{J_1+J_2+\mu R^2}\frac{\partial^2}{\partial\theta_1\partial\theta_2} + \frac{3\hbar^2}{8\mu R^2}\frac{(J_1+J_2)(J_1+J_2+2\mu R^2)}{(J_1+J_2+\mu R^2)^2}, \tag{2}$$

where

$$\mathcal{B}_{1(2)}(R)=\frac{J_{2(1)}+\mu R^2}{J_{1(2)}(J_1+J_2+\mu R^2)}\overset{R\to\infty}{\to}\frac{1}{J_{1(2)}}. \tag{3}$$

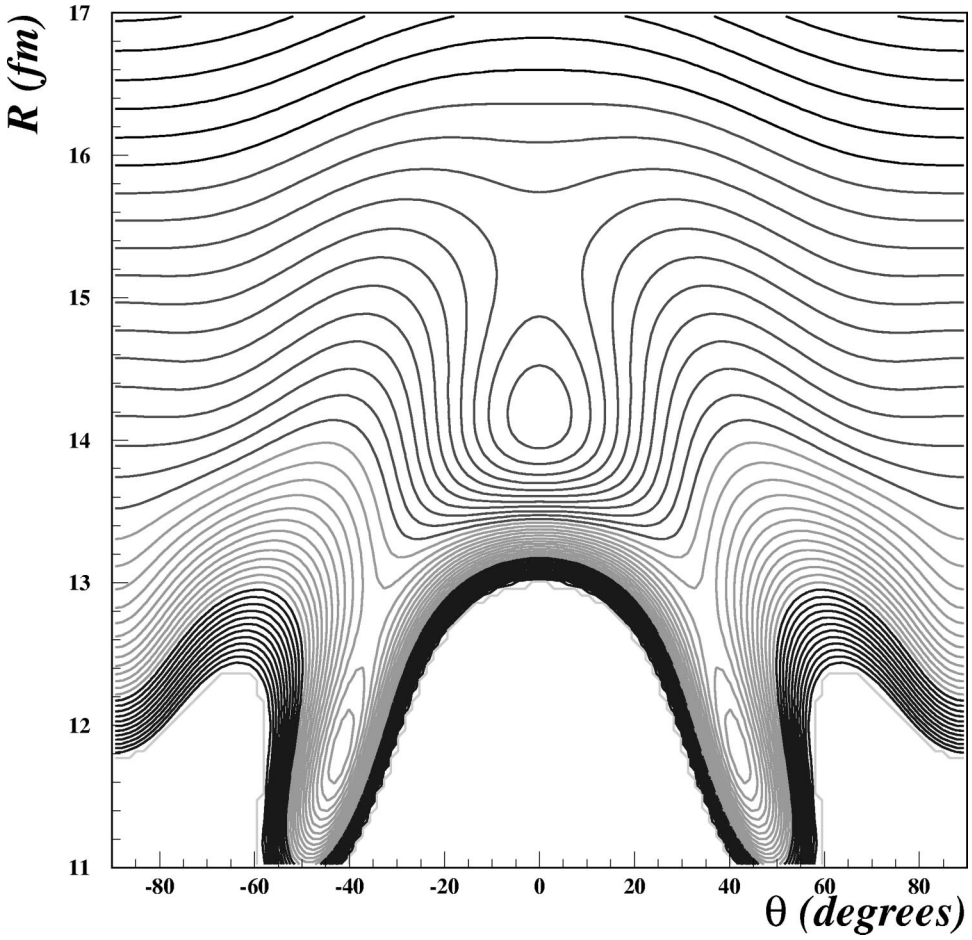

FIG. 2. Contour plots in $R-\theta$ variables of the total potential (5) for the splitting $^{252}\mathrm{Cf}\rightarrow{}^{148}\mathrm{Ba}+{}^{104}\mathrm{Mo}$. The lowest minimum is found for $\theta=0$ and $R=14.2$ fm.

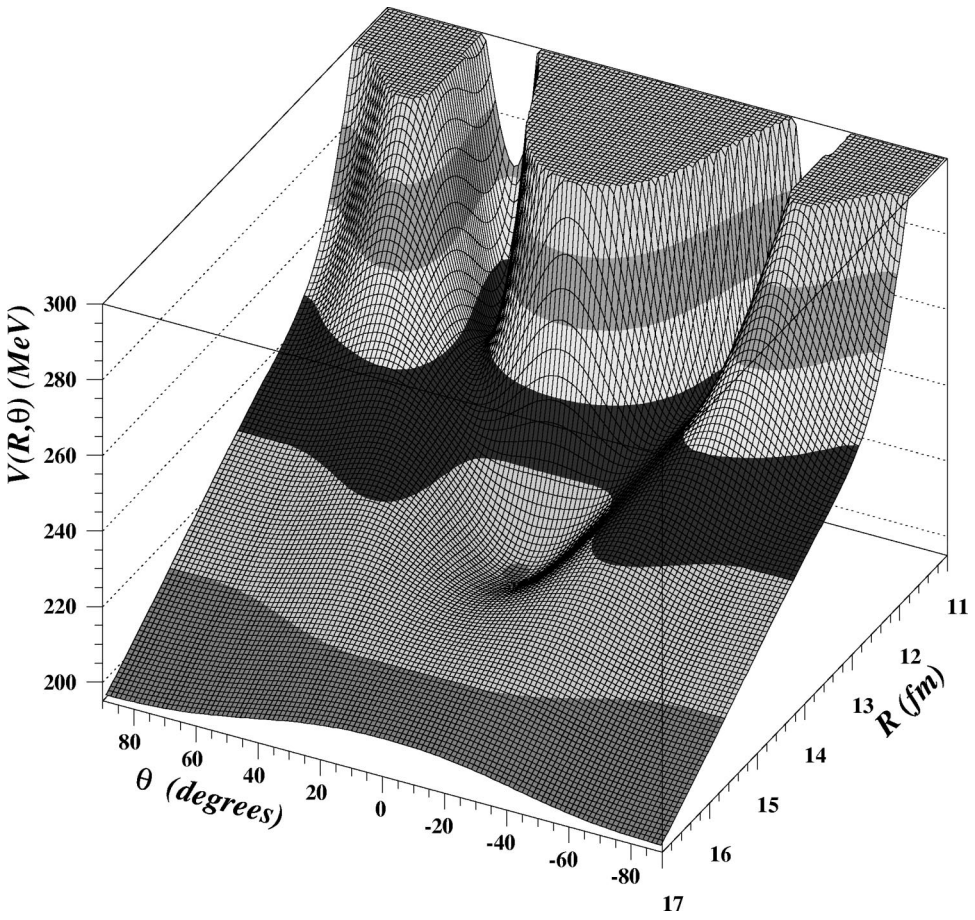

FIG. 3. The potential surface corresponding of the same case as in Fig. 2. The lowest barrier is encountered in the direction $\theta=0$.

As one can see the coupling between the three degrees of freedom is manifest. At this level some approximations can be done. First of all one has to note that in our cluster model the initially quasistationary state is confined inside a molecular pocket, limited on the left at approximately 13.5 fm by a highly repulsive wall arising from the compression term in the potential and on the right at approximately 14.5 fm by the Coulomb barrier. This fact can be visualized in Figs. 2–4. In Fig. 2, where we display the contour lines in radial-angular variables ($R-\theta \equiv \theta_1=\theta_2$) of the fragment-fragment potential, which is defined below, a molecular pocket is clearly developed in the direction of $\theta=0$. This case corresponds to the so-called *nose-to-nose* configuration when fragments are aligned along their symmetry axes. As one can see in Figs. 3 and 4, the minimum corresponding to the molecular pocket is also the deepest one, the other minimas, located off the symmetry are too high to accommodate metastable states of energy close or equal to the reaction Q value. In the above-mentioned range of R values, we have always $J_i \ll \mu R^2$. Consequently, we expand the Hamiltonian in powers of $J_i/\mu R^2$. In the first-order approximation, i.e., neglecting all terms directly proportional to $(\mu R^2)^{-2}$ or higher order, Eq. (2) rewrites

$$\hat{T}=-\frac{\hbar^2}{2\mu}\frac{\partial^2}{\partial R^2}-\frac{\hbar^2}{2J_1}\left(1-\frac{J_1}{\mu R^2}\right)\frac{\partial^2}{\partial\theta_1^2}$$
$$-\frac{\hbar^2}{2J_2}\left(1-\frac{J_2}{\mu R^2}\right)\frac{\partial^2}{\partial\theta_2^2}+\frac{\hbar^2}{\mu R^2}\frac{\partial^2}{\partial\theta_1\partial\theta_2}. \qquad (4)$$

We, therefore, deal with a multidimensional quantum system, in which the coordinate R is singled out as *collective* because it describes the relative nuclear motion. The other two coordinates $\theta_{1(2)}$ are usually called *intrinsic*.

The interaction between the nuclei composing the dinuclear molecule is taken according to our previous works (see [13], for example): A heavy-ion double folding integral where the effective nucleon-nucleon force is a sum of isoscalar and isovector M3Y and zero-range pseudoexchange interactions. In order to cope with the compression effects of the overlapping density a phenomenological repulsive potential was simulated by folding two density profiles with small diffuseness with a short-range effective force [14]. This short-range repulsive force is proportional to the overlapping volume. The strength of the repulsive term is fixed by requiring that the first resonant state in the molecular potential pocket coincides with the position of the Q value. We then obtain a molecular pocket that accommodates only one resonance. This requirement is consistent with our assumption that the cold fission is similar to the cluster radioactivity and α decay [15] and also agrees with the experiment that observes at infinity the emerging fragments with a maximal kinetic energy that is equal to the Q value. The double-folded potential is computed by making a general multipole expansion for two nuclei with distance R between their centers of mass and orientation given by the angles $\theta_{1,2}$ defined above (see the geometry of Fig. 1),

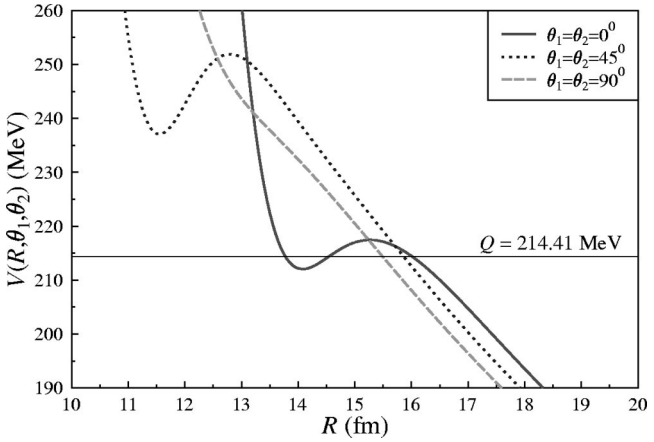

FIG. 4. The one-body potential for the cold splitting $^{252}\mathrm{Cf}\rightarrow{}^{148}\mathrm{Ba}+{}^{104}\mathrm{Mo}$ when $\theta_1=\theta_2=0°$ (thick-full curve), $\theta_1=\theta_2=45°$ (thick-dotted curve), and $\theta_1=\theta_2=90°$ (thick-dashed curve). The thin-full line at energy 214.41 MeV corresponds to the decay energy Q. The strength of the repulsive term was adjusted such that the first resonant state in the pocket along $\theta_1=\theta_2=0°$ coincides with Q.

$$V(R,\theta_1,\theta_2)=\sum_{\lambda_1,\lambda_2,\lambda_3}\frac{4\pi}{\sqrt{(2\lambda_1+1)(2\lambda_2+1)}}V^{\mu\ -\mu\ 0}_{\lambda_1\ \lambda_2\ \lambda_3}(R)\times Y_{\lambda_1\mu}(\theta_1,0)Y_{\lambda_2-\mu}(\theta_2,0). \tag{5}$$

In Fig. 4 we plotted the total potential (nuclear+Coulomb) for a selection of relative orientation angles. From the inspection of Fig. 4 one can infer again that the lowest barrier is obtained when $\theta_1=\theta_2=0$. Such an energetical argument supports the idea that the most likely fission trajectory in the binary case follows the path along the symmetry axes of the two fragments. As we had mentioned in Ref. [5] the dinuclear system is stable against small nonaxial fluctuations, which most likely are responsible for the formation of the fragments spins. Thence, for such small fluctuations, the potential in the region that is essential for tunneling can be expanded in the powers of the angles $\theta_{1,2}$,

$$V(R,\theta_1,\theta_2)=V(R,0,0)+\tfrac{1}{2}C_1\theta_1^2+\tfrac{1}{2}C_2\theta_2^2+C_{12}\theta_1\theta_2, \tag{6}$$

where the expressions of C_1 and C_2 (the fragment bending stiffness) and C_{12} (the coupling constant) are also given in Ref. [5].

The justification for such an approximation in the barrier region can be easily done by taking slices of the total potential in the direction perpendicular to the R axis. As one can see in Fig. 5, for small angles the potential in the perpendicular direction can be reasonably approximated with a harmonic curve. However, when the second turning point is reached at $R=16$ fm the potential becomes almost flat and the harmonic approximation no longer seems to be satisfactory. Thus, when the dinuclear system leaves the barrier, the fragments are no longer constrained in the perpendicular direction by a ''bound'' potential and are rotating under the action of the Coulomb torque.

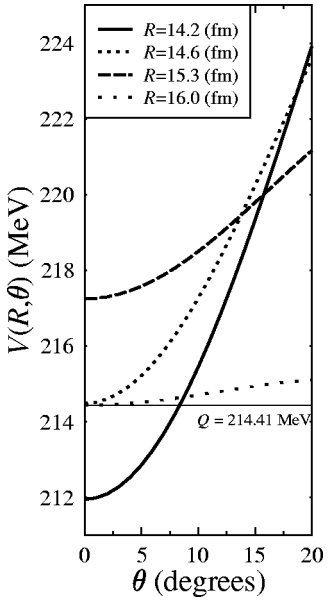

FIG. 5. Sections of the total potential along the transversal direction (θ axis) for different values of R.

A. Adiabatic approximation

The solution of the full quantum-mechanical problem in the variables $\boldsymbol{\theta}\equiv(\theta_1,\theta_2)$ and R,

$$(\hat{T}+\hat{V})\Psi(\boldsymbol{\theta},R)=E\Psi(\boldsymbol{\theta},R), \tag{7}$$

can be written by means of an expansion [16]

$$\Psi(\boldsymbol{\theta},R)=\sum_{n_1n_2}u_{n_1n_2}(\theta_1,\theta_2;R)v_\nu^{n_1n_2}(R), \tag{8}$$

based on the local adiabatic vibrational eigenfunctions $u_{n_1n_2}(\boldsymbol{\theta};R)$, depending parametrically on the tunneling coordinate R, and the quasistationary wave functions $v_\nu^{n_1n_2}(R)$ describing the fission mode. The eigenvalue problem of the bound motion reads

$$\hat{H}_{\mathrm{vib}}(\boldsymbol{\theta},R)u_{n_1n_2}(\boldsymbol{\theta};R)=\varepsilon_{n_1n_2}(R)u_{n_1n_2}(\boldsymbol{\theta};R), \tag{9}$$

where $\hat{H}_{\mathrm{vib}}(\boldsymbol{\theta},R)$ is given by

$$\hat{H}_{\mathrm{vib}}(\boldsymbol{\theta},R)=-\frac{\hbar^2}{2\mathcal{B}_1}\frac{\partial^2}{\partial\theta_1^2}-\frac{\hbar^2}{2\mathcal{B}_2}\frac{\partial^2}{\partial\theta_2^2}+\frac{\hbar^2}{\mu R^2}\frac{\partial^2}{\partial\theta_1\partial\theta_2}+\frac{1}{2}C_1\theta_1^2+\frac{1}{2}C_2\theta_2^2+C_{12}\theta_1\theta_2. \tag{10}$$

The eigenvalues of this Hamiltonian are labeled by the harmonic oscillator quantum numbers n_1 and n_2,

$$\varepsilon_{n_1n_2}(R)=\sum_{i=1}^{2}\hbar\Omega_i(R)\left(n_i+\frac{1}{2}\right), \tag{11}$$

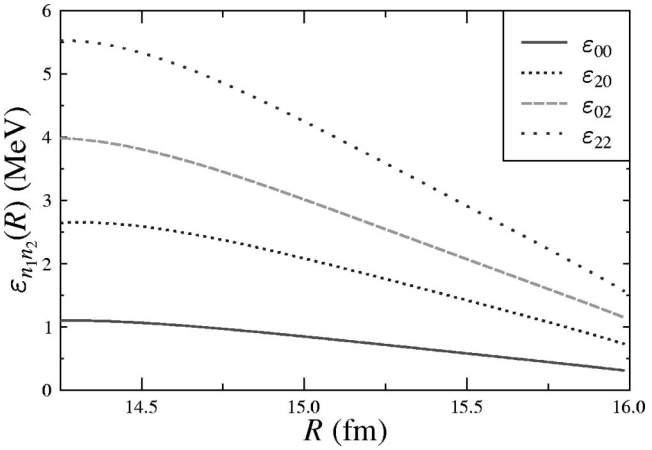

FIG. 6. Bending vibrations energy (11) as a function of the radial coordinate in the barrier region.

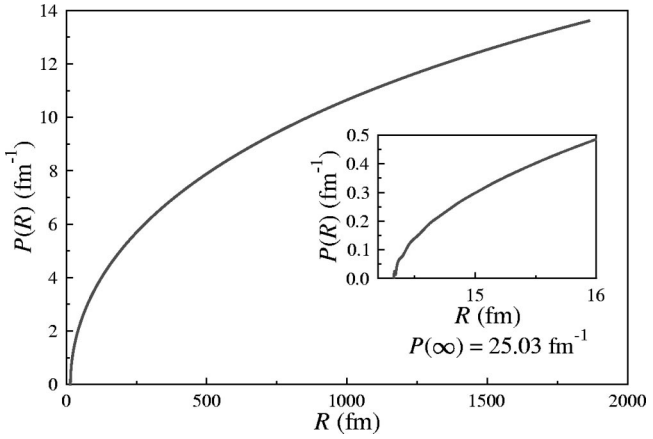

FIG. 7. Radial impulse of the dinuclear system as a function of the interfragment distance. The main picture describes the evolution of P_R up to the moment when it reaches its asymptotic value. In the inset we magnified the evolution of P_R only in the barrier's region.

where $\Omega_{1(2)}$ can be also found in Eq. (27) of Ref. [5] and the eigenfunctions are one-dimensional harmonic oscillators. The dependence of $\varepsilon_{n_1n_2}$ on R for different pairs of quantum numbers (n_1,n_2) is given in Fig. 6. The asymptotic limits of $\varepsilon_{n_1n_2}(R)$ as $R\to\infty$ should be in principle sums of nuclear bending vibrations energy. In the present case they will transform in rotational energies after the second turning point when the system is free to rotate.

Substituting Eq. (8) in Eq. (7) and using Eq. (9) we arrive at a set of coupled equations for the translational (fission) wave functions similar to the one considered in the past by other authors [17],

$$\left[-\frac{\hbar^2}{2\mu}\frac{\partial^2}{\partial R^2}+V(R)+\varepsilon_{n_1n_2}(R)-E\right]v_\nu^{n_1n_2} = \sum_{n_1'n_2'}\left(X_{n_1'n_2'}^{n_1n_2}\frac{\partial}{\partial R}+Y_{n_1'n_2'}^{n_1n_2}\right)v_\nu^{n_1'n_2'}, \tag{12}$$

where

$$X_{n_1'n_2'}^{n_1n_2}\equiv\frac{\hbar^2}{\mu}\left\langle u_{n_1'n_2'}\left|\frac{\partial}{\partial R}\right|u_{n_1n_2}\right\rangle,$$

$$Y_{n_1'n_2'}^{n_1n_2}\equiv\frac{\hbar^2}{2\mu}\left\langle u_{n_1'n_2'}\left|\frac{\partial^2}{\partial R^2}\right|u_{n_1n_2}\right\rangle. \tag{13}$$

The set of equations (12) provides the fission dynamics in the adiabatic representation, all coupling terms being due to the fission-mode kinetic energy. One should note that the channels that differ by an odd number of phonons, i.e., $n'=n\pm1,n\pm3,\ldots$, are not coupled. From the two types of coupling terms appearing in Eq. (12), $X_{n_1'n_2'}^{n_1n_2}$ are usually the most important, particularly as the decay energy increases, because the derivative $\partial/(\partial R)$ generates a term proportional to the radial (fission) momentum P_R. The physical significance of the nonadiabatic terms can be understood by considering the relative magnitudes of $|X_{n_1'n_2'}^{n_1n_2}(R)\partial/(\partial R)|$ and the level spacing $|\varepsilon_{n_1'n_2'}(R)-\varepsilon_{n_1n_2}(R)|$ [18]. Under semiclassical conditions the derivative $\partial/(\partial R)$ extracts the reduced momentum $P_R/\hbar$. Hence the condition necessary to neglect the terms on the right-hand side of Eq. (12) is that

$$\left|\frac{\langle u_{n_1'n_2'}|\partial/(\partial R)|u_{n_1n_2}\rangle\hbar v(R)}{\varepsilon_{n_1'n_2'}(R)-\varepsilon_{n_1n_2}(R)}\right|\ll1. \tag{14}$$

Consequently, the matrix element $\langle u_{n_1'n_2'}|\partial/(\partial R)|u_{n_1n_2}\rangle$ has the magnitude of the inverse of a distance δR related to the rate of change of $u_{n_1n_2}$ with R. Second, the level spacing $|\varepsilon_{n_1'n_2'}-\varepsilon_{n_1n_2}|$ may be used to define an R-dependent frequency component of the bending motion $\omega_{n_1'n_2'\to n_1n_2}(R)$. Thus the above inequality can be reduced to

$$|\delta R\,\omega_{n_1'n_2'\to n_1n_2}(R)/v(R)|\gg1, \tag{15}$$

showing that the time required to travel the distance δR at velocity $v(R)=1/\mu P_R$ must be sufficiently large to allow many periods of the bending motion.

According to Eq. (15), deviations from the adiabatic limit are expected to increase in importance for

(i) small $\delta R=1/\langle u_{n_1'n_2'}|\partial/(\partial R)|u_{n_1n_2}\rangle$ implying a rapid change in the composition of the bending oscillations wave function,

(ii) small $\omega_{n_1'n_2'\to n_1n_2}(R)$, implying a small level spacing $|\varepsilon_{n_1'n_2'}-\varepsilon_{n_1n_2}|$, and

(iii) large $v(R)$, implying a high fission velocity in the tunneling region.

In Fig. 7 we illustrate that (iii) is indeed not satisfied in the tunneling region, where the radial momentum P_R reaches up to 2% from the asymptotic value. This was expected because in the cold fission the prescission kinetic energy is almost nil [19]. The radial momentum P_R was determined by first solving the one-dimensional time-dependent Schrödinger equation (TDSE) for the variable R as described in

Ref. [20] and then computing the expectation value of the operator $-i\partial/\partial R$ at different moments of time. However, a departure from the adiabaticity condition (15), in conjunction with (ii), occurs when the dinuclear system approaches the end of the tunneling region. This can be easily seen in Fig. 8 where the validity of Eq. (15) is studied in the barrier's region. For the momentum we take the average value extracted from Fig. 7.

As for the lifetime of the resonant state in the radial one-dimensional potential, we obtain in the frame of the above-mentioned TDSE, for the splitting $^{252}\mathrm{Cf}\rightarrow{}^{148}\mathrm{Ba}+{}^{104}\mathrm{Mo}$, $T_{1/2}=1.3\times10^{-18}$ s. On the other hand, the calculated period of transversal oscillations $2\pi/\omega_{n_1'n_2'\rightarrow n_1n_2}(R)$ ranges between 3×10^{-21} and 2×10^{-20} s, and, therefore, the above-mentioned request that several oscillations are taking place during the tunneling is satisfied.

Accepting that the tunneling motion is well described in the adiabatic approximation the system of equations (12) will be decoupled. The additional potential $\varepsilon_{n_1n_2}(R)$ corrects the one-dimensional potential $V(R)$ for the changing amount of energy *frozen* in the bending degrees of freedom [21]. Thus, if the transversal degrees of freedom are completely decoupled, the monopolar part of the potential is modified only by a constant term.

A further improvement of this approximation may be obtained by the distorded-wave Born approximation (DWBA) of Eq. (12). Following Refs. [16,22] some simplifying assumptions can be made. As can be noticed from Fig. 4, essential for the description of the penetration through the barrier is the region between the two turning points (R_{t1} and R_{t2}) where the decay energy Q is intersecting the barrier. Then in the DWBA one can generalize the penetrability given in Eq. (30) of Ref. [16] as a function of the adiabatic one from one transversal degree of freedom to two degrees of freedom,

$$P_{\mathrm{DWBA}}=P_{\mathrm{adiab}}\left[1-\frac{\hbar}{4}\sum_{i=1}^{2}(n_i^2+n_i+1)\times\int_{R_{t1}}^{R_{t2}}dR\frac{\left(\frac{d\ln\lambda_i}{dR}\right)^2}{\sqrt{2\mu(V(R)+\varepsilon_{n_1n_2}(R)-Q)}}\right], \tag{16}$$

with $\lambda_i(R)=\sqrt{J_i\Omega_i(R)/\pi\hbar(1-J_i/\mu R^2)}$ and the adiabatic penetrability is evaluated simply with the Gamow formula.

B. Diabatic representation

The diabatic representation is obtained by expanding the total wave function in terms of a set of vibrational wave functions $\chi_i(\boldsymbol{\theta})$ most conveniently defined as the eigenfunctions of the vibrational Hamiltonian (10) at $R\rightarrow\infty$. In view of the above discussion on this asymptotic point, we chose as "infinity" the second turning point of the one-dimensional barrier in the R variable. Thus substituing the ansatz

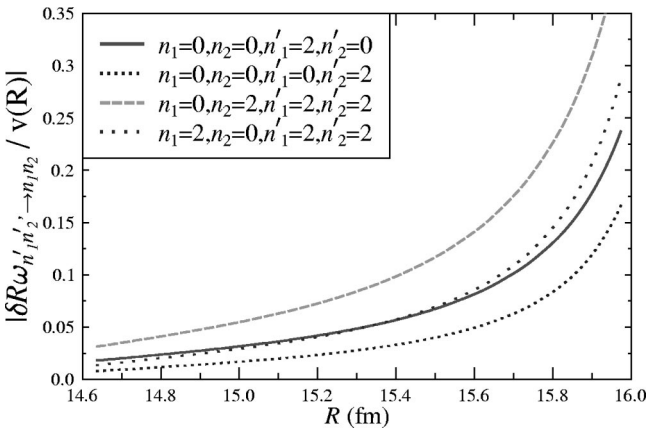

FIG. 8. The range of validity of the adiabaticity criterion as a function of R for the "molecular" transitions (20)→(00), (02)→(00), (22)→(20), and (22)→(02). At the left end of the barrier the criterion is safely fulfilled whereas at the right end it is less satisfactory.

$\Psi(\boldsymbol{\theta},R)=\Sigma_i\chi_i(\boldsymbol{\theta})\phi_i(R)$ in the eigenvalue problem (8) and taking as eigenvalue the decay energy of the corresponding cold fission reaction, we get the set of coupled-channels equations

$$-\frac{\hbar^2}{2\mu}\frac{\partial^2\phi_i}{\partial R^2}+[V(R)-Q]\phi_i=-\sum_j\langle\chi_j|\hat{H}_{\mathrm{vib}}|\chi_i\rangle\phi_j. \tag{17}$$

Under certain assumptions it is possible to simplify significantly this set of coupled-channels equations. In what follows we assume that the coupling interaction occurring in the right-hand side of Eq. (17) factors into a relative part, evaluated at the position of the unperturbed one-dimensional barrier ($R=R_b$), and an intrinsic part (see Ref. [23] and references therein),

$$\langle\chi_j|\hat{H}_{\mathrm{vib}}|\chi_i\rangle\cong\varepsilon_{ij}\delta_{ij}+\sum_{k=1}^{2}F_k(R_b)\langle\chi_j|G_k(\boldsymbol{\theta})|\chi_i\rangle. \tag{18}$$

In our case when the fission mode, described by the coordinate R, is coupled to two internal degrees of freedom, a quantum state is labeled by the harmonic oscillator numbers n_1 and n_2. In this case the formulas are lengthy and eventually we do not get less insight in the studied phenomenon if we limit ourselves to the case of butterfly vibrations that are a subclass of bending vibrations. Then the small angles θ_1 and θ_2 are approximately related [24],

$$q\equiv\theta_1\approx-\frac{R_2}{R_1}\theta_2, \tag{19}$$

where R_1 and R_2 are the fragments radii along the symmetry axes. We thus have the following expressions for the various quantities occurring in the coupling matrix (18):

$$\varepsilon_n=\frac{1}{2}\hbar\tilde{\omega}_0(R_\infty)\left(n+\frac{1}{2}\right)\left(\frac{\tilde{\mathcal{B}}(R_\infty)}{\tilde{\mathcal{B}}(R_b)}+\frac{\tilde{C}(R_b)}{\tilde{C}(R_\infty)}\right), \tag{20}$$

$$F(R_b)=\frac{1}{4}\hbar\tilde{\omega}_0(R_\infty)\left(\frac{\tilde{C}(R_b)}{\tilde{C}(R_\infty)}-\frac{\tilde{\mathcal{B}}(R_\infty)}{\tilde{\mathcal{B}}(R_b)}\right), \tag{21}$$

$$\langle\chi_{n'}|G(\theta)|\chi_n\rangle=\sqrt{n(n-1)}\,\delta_{n'n-2}+\sqrt{(n+1)(n+2)}\,\delta_{n'n+2}. \tag{22}$$

The meaning of different quantities occuring in the above formulas is given in Ref. [5].

For illustration we take three channels into account, e.g., $n=0$, 1, 2. Since according to Eq. (22) the channel with $n=1$ is not coupled to the other two channels, there will be no scattering of the initial $n=0$ state on an outgoing state with $n=1$ and, therefore, it will not contribute to the total penetrability. Equation (17) can be decoupled by means of a unitary transformation, as has been pointed out for fusion processes in Ref. [23],

$$\sum_{i,j} U_{ni}\langle\chi_j|\hat{H}_{\rm vib}|\chi_i\rangle U^{-1}_{jm}=\lambda_m\delta_{nm}. \tag{23}$$

The two eigenvalues of the matrix $\langle\chi_j|\hat{H}_{\rm vib}|\chi_i\rangle$ read

$$\lambda_{1,2}=\hbar\tilde{\omega}_0(R_\infty)\pm\sqrt{\hbar\tilde{\omega}_0(R_\infty)^2+2F^2}. \tag{24}$$

Thus every channel is now described by an independent Schrödinger equations, each of effective potential $V(R)+\varepsilon_0+\lambda_i$,

$$\left[-\frac{\hbar^2}{2\mu}\frac{\partial^2}{\partial R^2}+V(R)+\varepsilon_0(R_b)+\lambda_i(R_b)-Q\right]\sum_j U_{ij}\phi_j=0 \quad (i=1,2). \tag{25}$$

Then, using outgoing boundary conditions, i.e., $\phi_n \underset{R\to R_\infty}{\to} t_n e^{ik_nR}$ the total penetrability can be casted as a weighted sum of channels penetrabilities calculated at the shifted energies $Q-\varepsilon_0-\lambda_i$,

$$P(Q)=\sum_{i=1}^{2}|U_{i0}|^2P(Q-\varepsilon_0-\lambda_i). \tag{26}$$

This procedure can be easily extended to a larger number of channels, the difference being that the eigenvalues and the matrices performing the diagonalization of the coupling matrix are no longer available in a concise analytical form.

C. Path-integral approach

An alternative way to handle the problem is given by the path-integral formalism [23]. The tunneling probability can be obtained from the Feynman's transition amplitude, without resorting to the wave function as in the previously discussed approaches.

As we mentioned earlier, the problem considered in this paper, namely, the coupling between the fission mode and the bound transversal degrees of freedom represents a particular example of a multidimensional quantum mechanical system where the main collective degree of freedom (the translational fission mode) is coupled to intrinsic degrees of freedom (transversal modes). We define the intrinsic Hamiltonian $\hat{H}_{\rm intr}$ as the vibrational Hamiltonian from Eq. (10). This sub-Hamiltonian can be split further into a part $\hat{H}^0_{\rm intr}(\theta_1,\theta_2)$ that is independent on the collective coordinate R and the interaction $\delta\hat{H}_{\rm intr}(\theta_1,\theta_2;R)$ [25],

$$\hat{H}_{\rm intr}(\theta_1,\theta_2)=\hat{H}^0_{\rm intr}(\theta_1,\theta_2)+\delta\hat{H}_{\rm intr}(\theta_1,\theta_2;R). \tag{27}$$

In order to make the problem tractable, we evaluate $\hat{H}^0_{\rm intr}$ at a fixed value $R=R_b$, which is usually taken to be in the barrier region. Usually R_b is taken to be the position of the barier's top. Thus an expansion in the powers of R around R_b is performed,

$$\delta\hat{H}_{\rm intr}(\theta_1,\theta_2;R)=\left(\frac{\partial\hat{H}_{\rm intr}}{\partial R}\right)_{R=R_b}(R-R_b)+\frac{1}{2!}\left(\frac{\partial^2\hat{H}_{\rm intr}}{\partial R^2}\right)_{R=R_b}(R-R_b)^2+O[(R-R_b)^3]. \tag{28}$$

Like in the previous section we take the case of butterfly vibrations, when the nonaxial vibrations of the fragments composing the dinuclear system are in phase. We obtain the following expressions for the two parts of the intrinsic Hamiltonian in the intrinsic coordinate q:

$$\hat{H}^0_{\rm intr}(\theta_1,\theta_2;R)=-\frac{\hbar^2}{2\tilde{\mathcal{B}}}\frac{\partial^2}{\partial q^2}+\frac{1}{2}\tilde{\mathcal{B}}\tilde{\omega}_0^2q^2, \tag{29}$$

$$\delta\hat{H}_{\rm intr}(\theta_1,\theta_2;R)=-\frac{\hbar^2}{\mu R_b^2}\left(1-\frac{R_2}{R_1}\right)^2\left(1-\frac{3}{2R_b}(R-R_b)\right)\times(R-R_b)\frac{\partial^2}{\partial q^2}+\frac{1}{2}\left[\left(\frac{\partial\tilde{C}}{\partial R}\right)_{R=R_b}+\frac{1}{2}\left(\frac{\partial^2\tilde{C}}{\partial R^2}\right)_{R=R_b}(R-R_b)\right](R-R_b)q^2. \tag{30}$$

Introducing the creation and annihilation operators $\hat{a}$ and $\hat{a}^+$ for the harmonic oscillator the Hamiltonian becomes

$$\hat{H}_{\rm intr}=\hbar\tilde{\omega}_0(\hat{a}^+\hat{a}+\tfrac{1}{2})+[f(R)+g(R)](\hat{a}^+\hat{a}^++\hat{a}\hat{a})-[f(R)-g(R)](2\hat{a}^+\hat{a}+1), \tag{31}$$

where

$$f(R)=\frac{\hbar\tilde{\omega}_0}{4}\frac{\tilde{\mathcal{B}}}{\mu R_b^2}\left(1-\frac{R_2}{R_1}\right)^2\left(3\frac{R}{R_b}-5\right)\left(\frac{R}{R_b}-1\right),$$

$$g(R)=\frac{\hbar\tilde{\omega}_0}{4}\left[\left(\frac{\partial \ln\tilde{C}(R)}{\partial R}\right)_{R=R_b}+\frac{1}{2\tilde{C}(R)}\left(\frac{\partial^2\tilde{C}(R)}{\partial R^2}\right)_{R=R_b}(R-R_b)\right](R-R_b). \tag{32}$$

In the barrier region we checked numerically that $g(R)\gg f(R)$, which is mainly due to the large values of the relative inertia moment, i.e., $\mu R_b^2\gg\tilde{\mathcal{B}}$. Therefore, we can discard the terms multiplied by $f(R)$, which are coming from the vibrational kinetical part of Eq. (30). Consequently the form of the intrinsic Hamiltonian in the second quantization representation reads

$$\hat{H}_{\text{intr}}=[\hbar\tilde{\omega}_0+2g(R)](\hat{a}^+\hat{a}+\tfrac{1}{2})+g(R)(\hat{a}^+\hat{a}^++\hat{a}\hat{a}). \tag{33}$$

We then obtain a case similar to the example discussed in Ref. [26] for fusion. We consider the limiting case of *small frequency–large inertia*, when we let $\tilde{\omega}_0\to 0$ and $\tilde{\mathcal{B}}\to\infty$, which is approximately true when we approach the end of the barrier (see, for example, Fig. 6), simultaneously with $\tilde{\mathcal{B}}\tilde{\omega}_0=$ fixed. Accordingly, the penetrability for a given energy can be put in the following vivid integral form for a given decay energy [26]

$$P=\frac{1}{\sqrt{2\pi}}\int_{-\infty}^{+\infty}dx e^{-x^2/2}P_0[E,V(R)+x^2g(R)], \tag{34}$$

where P_0 is the one-dimensional penetrability in the variable R.

III. NUMERICAL RESULTS

In Fig. 9 we give the total penetrabilities in the adiabatic (P_{adiab}) and in the DWBA (P_{DWBA}) cases compared to the one-dimensional penetrability (P_0). We take into account up to four phonons, i.e., the maximum allowed excitation energy is ε_{22}. According to Fig. 6 the maximum of $\varepsilon_{22}<6$ MeV, i.e., it is in the vicinity of the neutron-emission threshold as one should have for the cold-fission reaction. In comparison to DWBA the adiabatic approximation overestimates the penetrability. One has to stress that the adiabatic approximation provides a correction of the penetrability only due to the zero-point energies of the transversal modes. In both cases the channel penetrability is reduced with increasing n_1,n_2 but the total penetrability $\Sigma_{n_1n_2}P_{n_1n_2}$ will be larger as compared to the one-dimensional case. In connection with this result one should recall the work of Brink *et al.* [27] which states that the penetrability computed for a Hamiltonian in which the intrinsic coordinate enters linearly in the coupling term satisfies the inequality $P\leqslant P_{\text{adiab}}$. In the case studied in this paper the coupling is quadratic in the intrinsic coordinate but the same inequality seems to work.

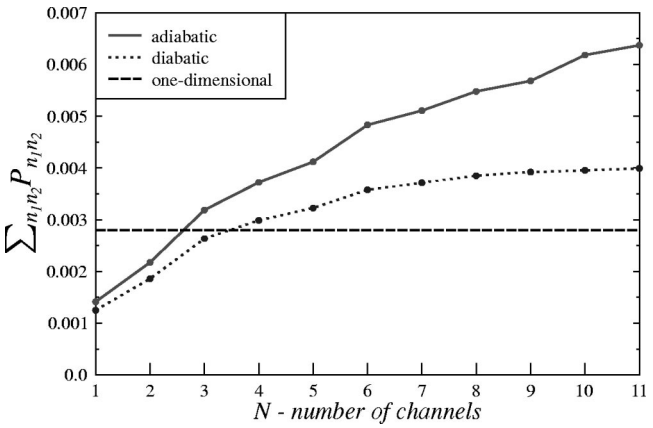

FIG. 9. Total penetrability $\Sigma P_{n_1n_2}$ as a function of the number of channels N.

As we mentioned above, in the adiabatic case, states with lower quantum numbers have larger tunneling probabilities. According to Ref. [28], where also a coupling quadratic in the vibrational coordinate is taken, by increasing the coupling strength, i.e., increasing the oscillations frequency or decreasing the mass inertia, and, therefore, moving towards the adiabatic limit, the most probable quantum state for the transmitted wave is the ground state. This is also in agreement to the result obtained in the present paper.

The diabatic coupling will provide values of the penetrability that are smaller as compared to the case when the main coordinate is not coupled. In Fig. 10 we plotted the penetrability computed with the help of Eq. (26) for different channels. For $n\geqslant 4$ we computed the eigenvalues and the elements of the unitary matrix $\hat{U}$ numerically. Figure 10 reveals the increase of the penetrability with the number of channels like in the adiabatic and DWBA approaches. The eigenchannels with effective energies $Q-\varepsilon_0-\lambda_i$ above the barrier's maximum were excluded from the sum (26). After taking into account eight channels we obtained a stable value of the penetrability.

For the barrier position we chose the unperturbed value,

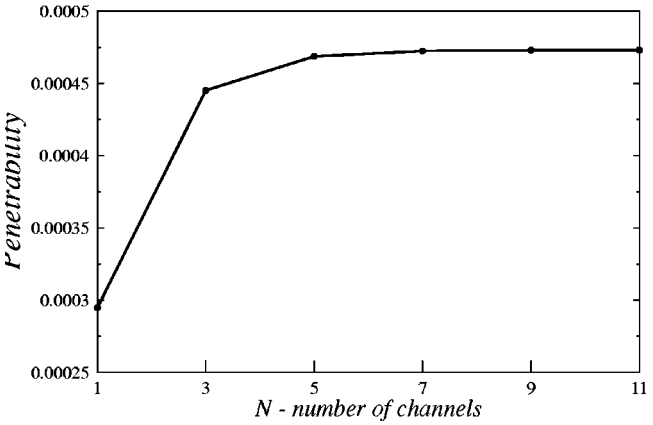

FIG. 10. Penetrability (26) as a function of the number of channels N.

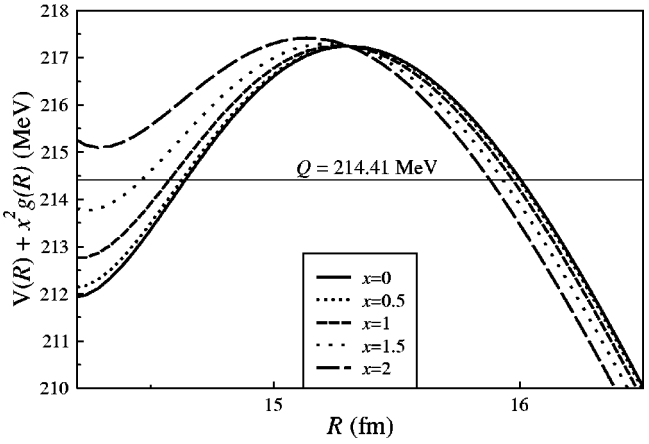

FIG. 11. The effective potential $V(R)+x^2g(R)$ occurring in the integral formula for the penetrability (34) for different values of x. For increasing x the barrier, i.e., the region bounded by the Q-value line and the potential, increases in height and width leading thus to an exponential decrease in penetrability.

i.e., $R_b=15.3$ fm, whereas for the asymptotic value, i.e., when the bending regime breaks down and the vibrational energy is transferred into rotations, we took $R_\infty=16$ fm, which is very close to the right end of the barrier (second touching point).

In order to see which range for the x variable, occurring in the integral formula (34), is essential, we draw in Fig. 11 the effective potential $V(R)+x^2g(R)$. As one can see for increasing x the barrier becomes thicker and higher and, therefore, the one-dimensional penetrability $P_0[V(R)+x^2g(R)]$ decreases. The integrand will be even more damped due to the presence of the gaussian exponential $\exp(-x^2/2)$. For values of x larger than a certain $x_{\rm cr}$, where the minimum of the potential intersects the Q-value line, $P_0=0$, because no metastable state of energy Q can be accomodated. Thus, the value of the integral can be safely determined for x in the range [0,1.5] for the given case. We get that $P(E)=5.94\times10^{-3}$ as compared to $P_0(E)=2.28\times10^{-3}$. Therefore, in the path integral approach, like in the adiabatic and DWBA treatments, the penetrability is increased as compared to the spherical case if we include several channels in the calculation. One should mention that the *small frequency–large inertia* is found at the other extreme in respect to the adiabatic case that corresponds to large frequencies [27].

IV. SUMMARY AND OUTLOOK

The main result of this paper is that in cold fission the coupling of the radial(fission) mode with the transversal molecular degrees of freedom tends to modify the penetrability. In the adiabatic, DWBA and *small frequency–large inertia* approximations the penetrability is increased as compared to the radial one-dimensional cases whereas in the diabatic it is lowered. However, we stress that these modifications are within the same order of magnitude and, therefore, are not affecting the lifetimes in a sensitive manner.

The fact that the tunneling time in the radial coordinate is larger by two orders of magnitude in comparison with the oscillation period of the transversal modes, enables us to apply the adiabatic Born-Oppenheimer approximation. In the adiabatic case the calculations are revealing a slow decreasing of the penetrability with the transversal oscillations quantum numbers. In the diabatic case we observe the same trend, i.e., the increase in the number of channels taken into account leads to a larger value of the penetrability. As we saw, the adiabatic approximation is less suitable when the tunneling path approaches the second turning point due to the gradual disapearence of the transversal barrier.

Concerning the above-mentioned aspect, i.e., that a large number of oscillations takes place during the tunneling motion, we would like to stress upon the fact that this makes possible the detection of these molecular-like collective states by γ deexcitation. As we saw in a previous paper [5] the account of these degrees of freedom is essential in establishing the fragments angular momentum.

It is also worthwhile to mention that in the case of cold fusion the coupling of the incident chanel to other channels can modify the barriers and lead to an enhanced fusion cross section below the barrier. However, in that case the coupling of the main tunneling mode, is made with degrees of freedom, other than the one considered by us in the case of cold fission. Moreover, the fragments considered in the present paper are sensitively deformed contrary to the case of fusion when the projectile is spherical or only weakly deformed.

ACKNOWLEDGMENTS

One of the authors (Ş.M.) would like to acknowledge the financial support from Alexander von Humboldt Stiftung. We are also grateful to Dipl. Phys. W. Krause for technical assistance.

[1] A. V. Ramayya, J. H. Hamilton, J. K. Hwang, and G. M. Ter-Akopian, in *Heavy Elements and Related New Phenomena*, edited by R. K. Gupta and W. Greiner (World Scientific, Singapore, 1999), Vol. I, p. 477.

[2] A. Săndulescu, Ş. Mişicu, F. Carstoiu, A. Florescu, and W. Greiner, Phys. Rev. C **57**, 2321 (1998).

[3] A. Săndulescu, A. Florescu, F. Carstoiu, W. Greiner, J. H. Hamilton, A. V. Ramayya, and B. R. S. Babu, Phys. Rev. C **54**, 258 (1996).

[4] G. M. Ter-Akopian *et al.*, in Proceedings of the Second International Conference Fission and Properties of Neutron-Rich Nuclei, Scotland, 1999, edited by J. H. Hamilton, W. R. Philips, and H. K. Carter, p. 246.

[5] Ş. Mişicu, A. Săndulescu, G. M. Ter-Akopian, and W. Greiner, Phys. Rev. C **60**, 034613 (1999).

[6] J. O. Rasmussen, W. Nörenberg, and H. J. Mang, Nucl. Phys. **A136**, 465 (1969).

[7] M. Zielinska-Pfabé and K. Dietrich, Phys. Lett. **49B**, 123 (1974).

[8] I. N. Mikhailov and P. Quentin, Phys. Lett. B **462**, 7 (1999).

[9] E. Uegaki and Y. Abe, Prog. Theor. Phys. **90**, 615 (1993).
[10] T. Banks and C. M. Bender, Phys. Rev. D **8**, 3346 (1973).
[11] U. Brosa, S. Grossmann, and A. Müller, Phys. Rep. **197**, 167 (1990).
[12] J. M. Eisenberg and W. Greiner, *Nuclear Theory, Vol. I: Nuclear Models* (North Holland, Amsterdam, 1987), p. 167.
[13] A. Săndulescu, Ş. Mişicu, F. Carstoiu, and W. Greiner, Fiz. Elem. Chastits At. Yadra **30**, 908 (1999) [Phys. Part. Nucl. **30**, 386 (1999)].
[14] P. O. Hess, Ş. Mişicu, W. Greiner, and W. Scheid, J. Phys. G **26**, 957 (2000).
[15] A. Săndulescu, Ş. Mişicu, A. Florescu, F. Cârstoiu, and W. Greiner, in Proceedings of the Second International Conference on Fission and Neutron-rich Nuclei, Scotland, 1999, edited by J. L. Durell and J. H. Hamilton, p. 59.
[16] H. Hofmann, Nucl. Phys. **A224**, 116 (1974).
[17] P. Ring, H. Massmann, and J. O. Rasmussen, Nucl. Phys. **A296**, 50 (1978).
[18] M-S. Child, *Molecular Collision Theory* (Academic, London, 1974).
[19] F. Gönnenwein and B. Börsig, Nucl. Phys. **A530**, 27 (1991).
[20] Ş. Mişicu, M. Rizea, and W. Greiner, J. Phys. G **27**, 993 (2001).
[21] J. Maruhn and W. Greiner, Phys. Lett. **44B**, 9 (1973).
[22] P. Ring, J. O. Rassmussen, and H. Massmann, Fiz. Elem. Chastits. At. Yadra **7**, 916 (1976) [Sov. J. Elem. Part. Nuclei **7**, 366 (1976)].
[23] A. B. Balatenkin and N. Takigawa, Rev. Mod. Phys. **70**, 77 (1998).
[24] P. O. Hess and W. Greiner, Nuovo Cimento A **83**, 76 (1984).
[25] B. Müller and N. Takigawa, Ann. Phys. (N.Y.) **173**, 163 (1987).
[26] A. B. Balatenkin and N. Takigawa, Ann. Phys. (N.Y.) **160**, 441 (1985).
[27] D. M. Brink, M. C. Nemes, and D. Vautherin, Ann. Phys. (N.Y.) **147**, 171 (1983).
[28] H. Massmann, K. Möhring, and P. Ring, J. Chem. Phys. **66**, 5368 (1977).